J Appl Electrochem (2007) 37:1429–1437
DOI 10.1007/s10800-007-9356-7

ORIGINAL PAPER

Influence of carbon support on the performance of platinum based oxygen reduction catalysts in a polymer electrolyte fuel cell

Jörg Kaiser · Pavel A. Simonov · Vladimir I. Zaikovskii · Christoph Hartnig · Ludwig Jörissen · Elena R. Savinova

Received: 7 October 2006 / Revised: 26 April 2007 / Accepted: 4 May 2007 / Published online: 13 July 2007

Abstract Novel carbons from the Sibunit family prepared via pyrolysis of hydrocarbons [Yermakov YI, Surovikin VF, Plaksin GV, Semikolenov VA, Likholobov VA, Chuvilin AL, Bogdanov SV (1987) React Kinet Catal Lett 33:435] possess a number of attractive properties for fuel cell applications. In this work Sibunit carbons with BET surface areas ranging from ca. 20 to 420 m^2 g^{-1} were used as supports for platinum and the obtained catalysts were tested as cathodes in a polymer electrolyte fuel cell. The metal loading per unit surface area of carbon support was kept constant in order to maintain similar metal dispersions (~0.3). Full cell tests revealed a strong influence of the carbon support texture on cell performance. The highest mass specific activities at 0.85 V were achieved for the 40 and 30 wt.% Pt catalysts prepared on the basis of Sibunit carbons with BET surface areas of 415 and 292 m^2 g^{-1}. These exceeded the mass specific activities of conventional 20 wt.% Pt/Vulcan XC-72 catalyst by a factor of ca. 4 in oxygen and 6 in air feed. Analysis of the I–U curves revealed that the improved cell performance was related to the improved mass transport in the cathode layers. The mass transport overvoltages were found to depend strongly on the specific surface area and the texture of the support.

Keywords Carbon support · Oxygen reduction · PEMFC · Platinum catalyst

J. Kaiser · C. Hartnig · L. Jörissen
Division 3 Electrochemical Energy Storage and Conversion, Center for Solar Energy and Hydrogen Research, Baden-Württemberg, Helmholtzstrasse 8, 89081 Ulm, Germany

J. Kaiser (✉)
Degussa-Initiators GmbH & Co. KG, Dr.-Gustav-Adolph-Str. 3, 82049 Pullach, Germany
e-mail: joerg.kaiser@degussa.com

P. A. Simonov · V. I. Zaikovskii · E. R. Savinova
Boreskov Institute of Catalysis, Russian Academy of Sciences, Pr. Akademika Lavrentieva 5, Novosibirsk 630090, Russia

1 Introduction

Low temperature fuel cells (FC), based on proton exchange membranes driven with either hydrogen (PEMFC) or alcohols (DMFC, DAFC) are promising energy sources for mobile and portable applications. However, their commercial use is still limited due to high costs and insufficient durability [1, 2]. Recently considerable effort has been directed towards the optimization of the active component of electrocatalysts. Less attention has however been paid to the improvement of the catalyst supports. Meanwhile, substructural characteristics of carbon materials (porosity, specific surface area, texture, nanostructure, and surface properties) exert a strong influence on the: (i) size and morphology of metal nanoparticles, (ii) catalyst stability, (iii) metal/ionomer contact and catalyst utilization, (iv) mass-transport, and (v) water management, and hence may be a key issue for the FC performance. The critical dependence of the fuel cell performance on the microstructure and porosity of the catalyst layers has already been outlined in a number of publications [3–8]. Recognition of the importance of the carbon support properties has recently motivated a number of research groups to employ various novel carbon supports, such as carbon nanotubes [9], nanofibers [10–12] and mesoporous carbons [13, 14] for FC applications. However, no systematic approach has been employed so far to the investigation of the influence of catalyst supports on cell performance.

Recently Rao et al. [15] studied the influence of the carbon support on the fuel cell performance at constant metal dispersion in order to avoid overlapping effects of the support on the metal dispersion on the one hand and on reaction macrokinetics in the catalyst layer on the other hand. They used a series of PtRu catalysts with practically identical metal dispersion supported on proprietary carbon materials of the Sibunit family [16] prepared via pyrolysis of hydrocarbons with BET surface areas from ca. 6 to 415 $m^2\ g^{-1}$. The different combinations were tested in a liquid fed DMFC. The mass and specific activity of PtRu anode catalysts was found to increase dramatically with decreasing BET surface area of the support. Catalysts supported on low surface area carbon showed superior mass specific activities, exceeding that of the commercial Vulcan XC-72 PtRu catalyst by nearly a factor of 3.

In a hydrogen fuelled PEMFC voltage losses are dominated by cathodic overvoltages. Considering the superior performance of DMFC anode catalysts based on carbon materials of the Sibunit family, we tested Sibunit carbons with BET surface areas ranging from ca. 20 to 420 $m^2\ g^{-1}$ as supports for PEMFC cathode catalysts in this work. The incentive was on the one hand to learn more about the influence of the carbon support porosity on the cathode performance and on the other hand to explore the potential of Sibunit carbons for PEMFC cathode catalysts.

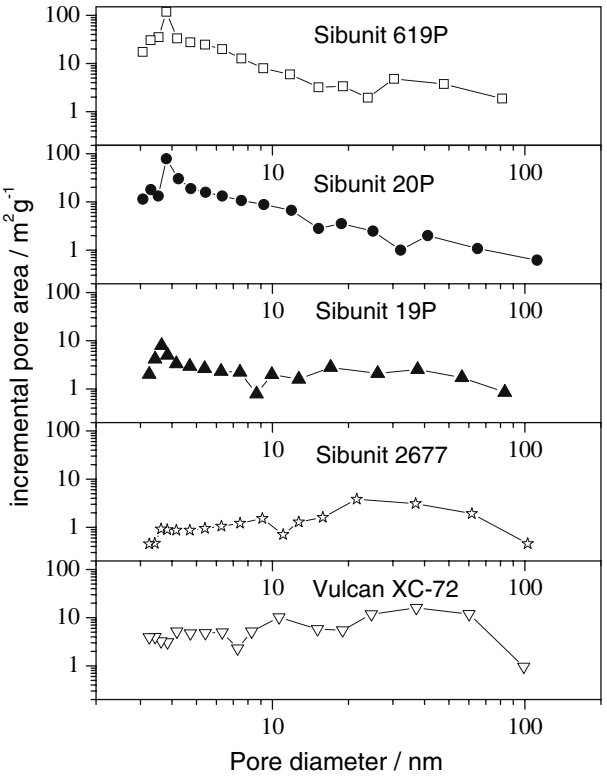

Fig. 1 Pore size distributions for carbon materials utilized in this work obtained from BJH desorption method [17]

2 Experimental

2.1 Catalyst preparation

Carbons of the Sibunit family (Omsk, Russia) with BET surface areas ranging from 22 to 415 $m^2\ g^{-1}$ and Vulcan XC-72 (210 $m^2\ g^{-1}$, Cabot Corp.) were used as catalyst supports. Textural characteristics were obtained from nitrogen adsorption measurements at 77 K (ASAP 2400, Micrometrics). For further details the reader is referred to [15]. Pore size distribution curves are shown in Fig. 1.

The preparation of Pt/C catalysts consisted of a number of steps. First, carbon materials were milled down to 2–5 μm. Then its aqueous suspension in 0.2 M H_2PtCl_6 was prepared at 20 °C under vigorous stirring and heated up to 80 °C. Next, NaOOCH was added drop-wise to the suspension of carbon at 80 °C. The value of pH was maintained between 6 and 7 by addition of Na_2CO_3. The slurry was stirred for 1 h, cooled and filtered. The resulting deposit was washed with distilled water until the reaction with aqueous $AgNO_3$ was negative, dried in vacuum at 100 °C and reduced in a H_2 stream. The characteristics of the catalysts obtained are listed in Table 1.

High-resolution transmission electron microscopy (HRTEM) images were obtained with a JEM-2010 microscope (JEOL, Japan) with a lattice-fringe resolution of 0.14 nm at an accelerating voltage of 200 kV. Samples for HRTEM were prepared on a perforated carbon film mounted on a copper grid. Metal particle size distributions (PSDs) were obtained from TEM images and used to calculate average diameters of metal particles $\overline{d} = \sum_i n_i d_i / \sum_i n_i$.The metal dispersion (D) of the Pt/C catalysts was calculated using data of pulse CO chemisorption in H_2 at 20 °C, assuming that each Pt surface atom adsorbs one CO molecule.

2.2 Fuel cell testing

Electrodes of $5 \times 5\ cm^2$ were prepared by the spraying method [18, 19] and used for PEMFC tests. The corresponding catalyst inks were prepared by stirring an appropriate amount of catalyst and Nafion® (equivalent weight 1,100 g mol^{-1}, 15 wt.% solution) and 5 ml of deionized water. Nafion 112 purchased from IonPower Inc. was used as a membrane. An E-TEK Pt/C (40 wt.% Pt) catalyst at a metal loading of 0.4 $mg_{Pt}\ cm^{-2}$ was applied at the anode. In order to minimize variations in the thickness and thus mass transport related losses, the cathode carbon loading (rather than the metal loading) was kept constant at ~0.6 $mg_C\ cm^{-2}$. The Nafion® content was 17 wt.% for all

Table 1 Characteristics of the cathode catalysts

Catalyst	40%Pt/Sibunit 619P	30%Pt/Sibunit 20P	10%Pt/Sibunit 19P	10%Pt/Sibunit 2677	20%Pt/Vulcan XC-72
S_{BET} of carbon support/m^2 g^{-1}	415	292	72.3	21.9	210
Pt loading/μmol m^{-2}	8.24	7.53	7.88	26.0	5.99
Pt dispersion, CO/Pt	0.175	0.245	0.295	0.185	0.27
Pt specific surface area/m^2 g^{-1}	49.6	69.5	83.7	52.5	76.6
Mean particle diameter/nm	2.7	2.7	2.0	3.0	2.7

Table 2 Characteristics of the cathode layers of the MEAs[a]

Catalyst	40%Pt/Sibunit 619P	30%Pt/Sibunit 20P	10%Pt/Sibunit 19P	10%Pt/Sibunit 2677	20%Pt/Vulcan XC-72
Pt loading/mg_{Pt} cm^{-2}	0.39	0.25	0.06	0.06	0.15
Carbon loading/mg_C cm^{-2}	0.59	0.59	0.58	0.56	0.59
Nafion loading/mg_{Nafion} cm^{-2}	0.21	0.18	0.14	0.13	0.15
Nafion loading per m^2 of carbon support/mg_{Nafion} m^{-2}	0.86	1.04	3.34	10.6	1.01

[a] For all MEAs Nafion 112 was used as a membrane, E-TEK Pt/C (40 wt.%) at 0.4 mg_{Pt} cm^{-2} as an anode; Nafion content in all cathodes: 17 wt.%

cathodes. Characteristics of the cathode layers of the membrane electrode assemblies (MEAs) are listed in Table 2. Gas diffusion layers from SGL Carbon, type Sigracet 10BB (5% PTFE hydrophobized, single side coated with a microporous layer), were assembled together with the catalyst coated membrane into a single graphite test cell provided by Electrochem, Inc. This was designed with identical flow fields at the anode and cathode, having one inlet and one outlet connected by 5 parallel channels.

Current voltage (I–U) curves were recorded galvanostatically at 60 °C with humidified hydrogen (dew point 60 °C) as anode feed and humidified air or oxygen (dew point 55 °C) as cathode feed, both gases supplied to the cell at ambient pressure. Before recording the I–U curve from high to low currents, the cell was equilibrated at the maximum current of the I–U curve until the cell voltage, the cell resistance, and the temperatures of the gases at the cell inlet and the cell outlet were constant for at least 15 min (the cell operated stably once these conditions were met).

3 Results and discussion

3.1 Characterization of Pt/C catalysts

Carbons of the Sibunit family are prepared through pyrolysis of natural gases on carbon black surfaces (templates) followed by an activation step to achieve desired values of the surface area and pore volume [16]. Pyrolysis leads to formation of dense graphite-like deposits on the surface of the carbon black. In the course of activation the carbon black component undergoes gasification, with its extent depending on the conditions and the duration of the activation step. Hence, the PSD in the resulting Sibunit sample roughly reproduces the PSD in the carbon black precursor. Variation of the type of the gas source, the template (carbon black), and the manner and duration of the activation, results in meso- to macroporous carbon materials with specific surface areas from 1–50 (non-activated) to 50–500 m^2 g^{-1} (activated) and pore volumes of up to 1 cm^3 g^{-1}. This gives a unique opportunity to vary the specific area of carbon supports, keeping their chemical nature essentially intact. Other advantages of carbons of the Sibunit family are: (i) purity, (ii) high electrical conductivity, (iii) uniform morphology of primary carbon globules (contrary to carbon blacks, in particular Vulcan [20]), and (iv) high mechanical hardness. Note that the latter affects microstructure and secondary porosity of the catalytic layers.

In order to investigate the influence of carbon support porosity on the performance of a PEMFC cathode, four carbon materials from the Sibunit family with BET surface areas ranging from ca. 20 to more than 400 m^2 g^{-1} were tested along with Vulcan XC-72 which was used as a reference. Characteristics of the different carbon materials are listed in Table 1. The extent of activation increased

from Sibunit 2677 (no activation) to 19P, 20P, and then to 619P. Figure 1 shows the incremental pore area distributions obtained from the BJH desorption method [17]. The latter demonstrate that an increase of the activation degree results in an augmentation of the contribution of pores below 20 nm in diameter.

In order to produce catalysts with similar metal dispersions and thus avoid an influence of the particle size on the catalytic activity of Pt in the oxygen reduction reaction (ORR) observed in previous work and widely discussed in the literature [21–25], the amount of Pt per unit surface area of carbon support was maintained in the range between 6 and 8 μmol m^{-2} (except for Sibunit 2677 where the Pt loading was higher). The resulting values of Pt dispersion were close to the target value 0.3 for Sibunit 19P, 20P, and Vulcan XC-72 samples, but were considerably lower for Sibunit 2677 and 619P (see Table 1). Similar values of Pt loadings and dispersions lead to similar interparticle distances, which are of relevance for processes occurring in the mixed or diffusion-controlled regime.

Electron microscopy revealed that all samples consisted of highly dispersed Pt nanoparticles with an average particle size around 3 nm evenly distributed along the support surface (Figs. 2, 3) but also contained some rough metal particles ca. 10–15 nm in size. The latter contributed to a decrease in the metal dispersion for the 40%Pt/Sibunit 619P and 10%Pt/Sibunit 2677 catalysts. Formation of metal particles strongly differing in size and location on carbon support is usually related to the co-existence of several pathways for their formation [26]. The genesis of Pt particles during catalyst preparation may occur through different mechanisms, namely: (i) spontaneous reduction of H_2PtCl_6 by carbon via the "electrochemical" mechanism resulting in rough particles [26] and (ii) hydrolysis of platinum chloride and reduction of its chlorooxocomplexes to metal particles in Na_2CO_3 + NaOOCH medium leading to a highly dispersed phase. Further investigations are required to prevent formation of large particles and to make the catalysts more uniform.

3.2 Oxygen reduction in a PEMFC

Current–voltage curves recorded at 60 °C and corrected by the ohmic drop (the real part of the impedance of the 1,000 Hz ac signal, typically in the range of 0.125 Ω cm^2, measured for each data point separately) are displayed in Fig. 4a and b measured for air and oxygen feed, respectively. Since the carbon loading was in all cases equal to 0.6 mg_C cm^{-2} and with the metal percentage on the carbon support being different, the metal loadings in the cathodes varied from 0.06 mg_{Pt} cm^{-2} (10%Pt/Sibunit 19P, 10%Pt/Sibunit 2677) to 0.39 mg_{Pt} cm^{-2} (40%Pt/Sibunit 619P) (see Table 2). Given these different Pt loadings, the divergence of the I–U curves and the increase in the overpotential with decreasing platinum content is not surprising. We would like to emphasize the following observations: First, the difference in the I–U curves for 40%Pt/Sibunit 619P and 30%Pt/Sibunit 20P is surprisingly small given the difference in Pt loading of a factor of 1.56. Second, the I–U curves for Pt supported on Vulcan XC-72 and 10%Pt/Sibunit 19P nearly coincide in the low overpotential interval (kinetic region) although the metal loading in the former case is 2.5 times higher. Note that CO chemisorption results in similar values of Pt dispersion for

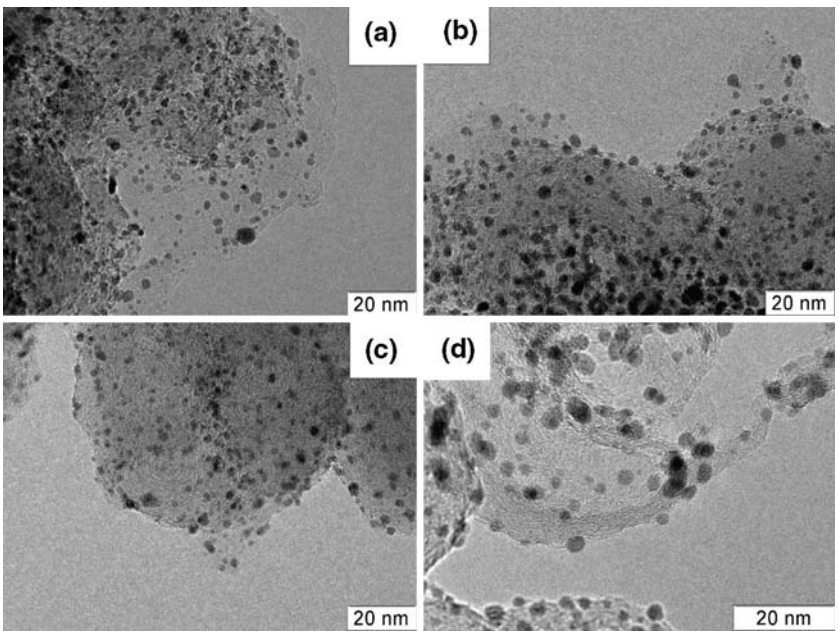

Fig. 2 TEM images of Pt/C samples: (**a**) 10%Pt/Sibunit 19P, (**b**) 10%Pt/Sibunit 2677, (**c**) 30%Pt/Sibunit 20P, (**d**) 40%Pt/Sibunit 619P

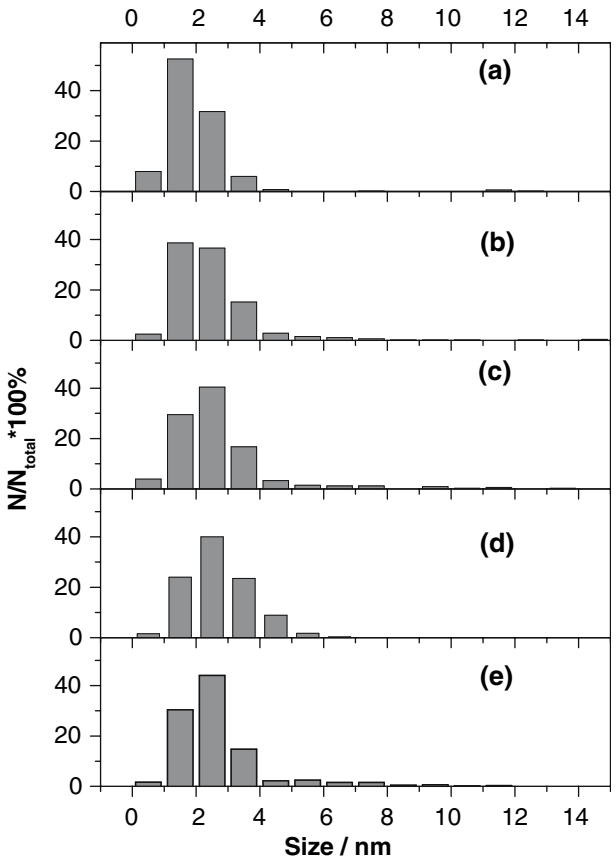

Fig. 3 Particle size distributions for Pt/C samples: (**a**) 10%Pt/Sibunit 19P, (**b**) 10%Pt/Sibunit 2677, (**c**) 30%Pt/Sibunit 20P, (**d**) 40%Pt/Sibunit 619P, (**e**) 20%Pt/Vulcan XC-72

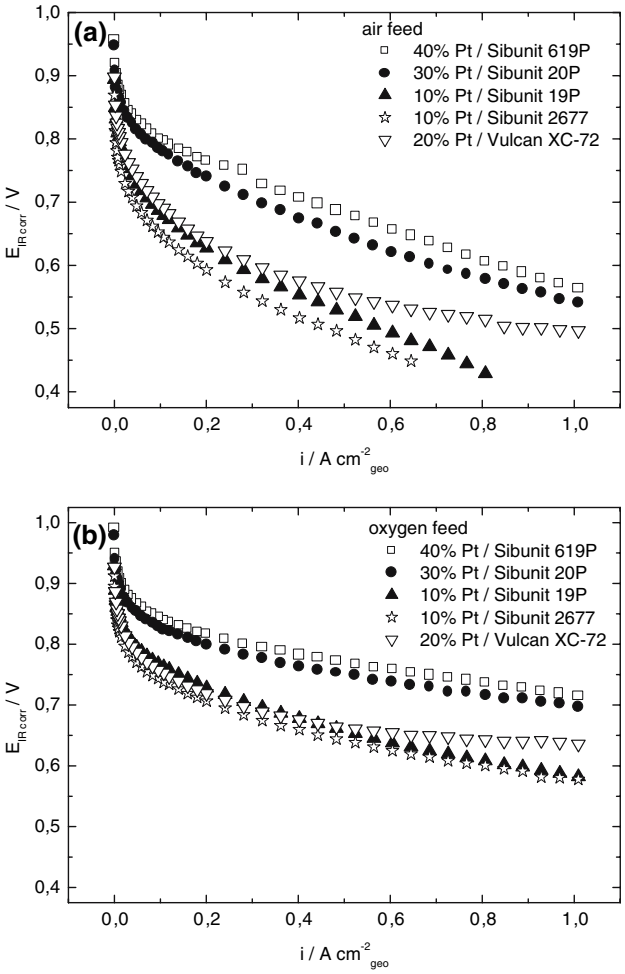

Fig. 4 IR corrected I–U curves with air (**a**) and with oxygen (**b**) feed on the cathode side. T_{cell} = 60 °C, anode: H_2 feed, Pt/C, 0.4 mg_{Pt} cm^{-2}, $\lambda = 2$ for $i \geq 0.2$ A cm^{-2}, dp 60 °C, ambient pressure; cathode: Pt/C, 0.6 mg_C cm^{-2}, $\lambda = 4$ for air feed and $\lambda = 5$ for oxygen feed for $i \geq 0.2$ A cm^{-2}, dp 55 °C, ambient pressure

20%Pt/Vulcan XC-72 and 10%Pt/Sibunit 19P catalysts (Table 1). These observations point to a strong influence of the texture of the carbon support on the cathode performance and to superior properties of carbons of the Sibunit family compared to Vulcan XC-72.

More information can be gained from the comparison of the mass specific activities (MA) in the kinetic region which are plotted in Fig. 5a and b for air and oxygen fed fuel cells. The MA of an oxygen fed cathode is the lowest for 20%Pt/Vulcan XC-72 and the highest for 30%Pt/Sibunit 20P. The MAs achieved in this work are comparable (considering lower operation temperature) to state of the art activities of PEMFC cathodes [25]. The ratio of MAs for the most active and the least active sample amounts to 3.4 at 0.8 V and to 4.2 at 0.85 V, and is thus even greater than the difference in the MAs observed by Rao et al. [15] for methanol oxidation. However, in contrast to [15], in this work MAs do not scale with the BET surface area of carbon supports. For example, PtRu catalysts supported on Sibunit 20P and Vulcan XC-72 with similar BET surface areas (Table 1) showed very similar MAs at the anode of a DMFC [15], while Pt catalysts based on these supports reveal very different MAs at the cathode of a PEMFC (Fig. 5). It is interesting to mention that in air fed fuel cells the activity ranking changes. While Pt supported on Sibunit 20P still demonstrates the highest MA, the lowest activity is now observed for the 10%Pt/Sibunit 2677 sample with the lowest BET surface area of 22 m^2 g^{-1}. The ratio between the most active and the least active sample with air feed is even greater than with oxygen and amounts to 5.1 at 0.8 V and to 6 at 0.85 V.

Various factors might cause the observed influence of carbon on the MA, in particular: (i) metal dispersion, (ii) metal–support interaction, (iii) support–ionomer interaction and catalyst utilization factor, (iv) mass transport, and (v) water management. We will further analyze which of these are likely to explain the results of this work.

According to the results of gas-phase CO chemisorption, specific surface areas of Pt in this work ranged from ca. 50

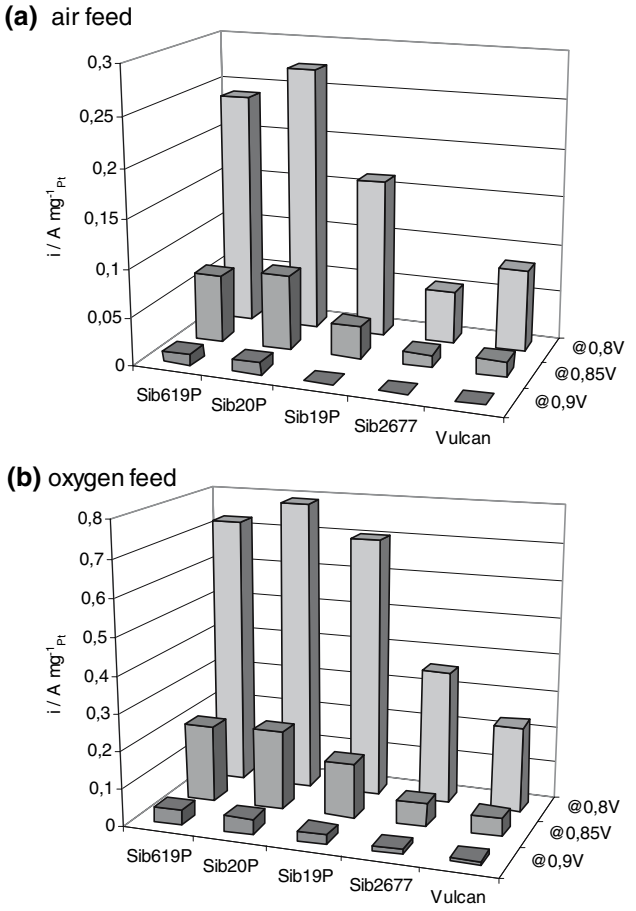

Fig. 5 Comparison of mass specific, IR corrected activities for Pt cathode catalysts prepared on the basis of various carbon materials at different cell voltages for air (**a**) and oxygen (**b**) fed PEMFC

to 80 $m^2\ g^{-1}$ (Table 1). The analysis carried out in [25] showed that MA of Pt in the ORR does not change substantially in this interval of specific surface areas. Strong differences in the MAs due to the metal-support interactions are rather unlikely, since, on the one hand, supports utilized in this work belong to the same family (except for the reference Vulcan XC-72 sample) and thus have similar interfacial properties, and, on the other hand, carbon materials are known to interact with Pt rather weakly [27].

The catalyst utilization factor may indeed depend strongly on the carbon support morphology as pointed out by Rao et al. [15]. In fact, for the same series of carbon materials the catalyst utilization factor has been found to increase with decreasing BET surface area (S_{BET}) of carbon. Unfortunately, in this work we did not succeed in accurately determining metal utilization factors for samples with low Pt content and hence low absolute Pt surface area, since evaluation of the electrochemically active surface areas (EASA) through CO stripping or hydrogen underpotential deposition was hindered by hydrogen crossover from the anode to the cathode. However, a rough estimation of the EASA by CO stripping indicated that the decrease in the catalyst utilization factor with S_{BET} observed by Rao et al. for the same carbon materials did not occur in this work. This may be tentatively ascribed to different procedures for the preparation of the catalytic layers employed in [15] and in this work. In particular, in [15] the catalyst ink was prepared in water–isopropanol mixture, while in this work water was used as a solvent. Meanwhile, as pointed out by Uchida et al. [5] and by Lundblad [28], the ionomer penetration in the primary (between particles in carbon agglomerates) and secondary (between carbon agglomerates) pores and thus its distribution in the catalyst layer crucially depends on the type of solvent.

Mass transport and water management in the catalyst layer seem to be the most likely reasons for the influence of the carbon support porosity on the cathode performance observed in this work. This hypothesis is supported by the differences in the mass activities observed in the oxygen and air feed (Fig. 5a, b). For a more detailed analysis we consider various contributions to the voltage losses.

In general, the cell voltage E_{cell} can be represented as a difference between the reversible potential of the cell reaction E_{rev} [29] and the sum of kinetic overvoltages ($\eta_{kin,an}$ and $\eta_{kin,cat}$), mass transport overvoltages ($\eta_{mt,an}$ and $\eta_{mt,cat}$) and ohmic drop ($\eta_{ohm} = I^*R$) [25]:

$$E_{Cell} = E_{rev} - \left(\eta_{kin,an} + \eta_{kin,cat} + \eta_{mt,an} + \eta_{mt,cat} + \eta_{ohm}\right). \quad (1)$$

Here we neglect hydrogen crossover since its contribution was below 1 mA cm^{-2}_{geo}. For a Pt anode at a fairly high loading of 0.4 $mg_{Pt}\ cm^{-2}$, which is fed with pure hydrogen at a utilization of 50%, kinetic and mass transport overvoltages may be neglected, at least for small and medium current densities. This simplifies the analysis and allows to estimate mass transport losses at the cathode with Eq. (2):

$$\eta_{mt,cat} = E_{rev} - E_{cell} - \eta_{kin,cat} - \eta_{ohm}. \quad (2)$$

The cell resistance R was measured from the impedance data (see above). Kinetic overvoltages for the ORR may be accessed through Tafel analysis [25] of the kinetic interval of the I–U curves. Figure 6 shows the IR corrected cell voltages in the range from 0.001 to 0.01 A cm^{-2}_{geo} with the corresponding regression lines ($E = E' + b * \log i_0 - b * \log i$ [30]) showing the Tafel behavior of the data points in this current region. Above 0.01 A cm^{-2}_{geo}, the data points were already deviating slightly from linear behavior thus indicating that mass transport losses influence the cell voltage even at small current densities. This is not necessarily related to poor cathode structures but rather to the operating conditions (ambient cell pressure and

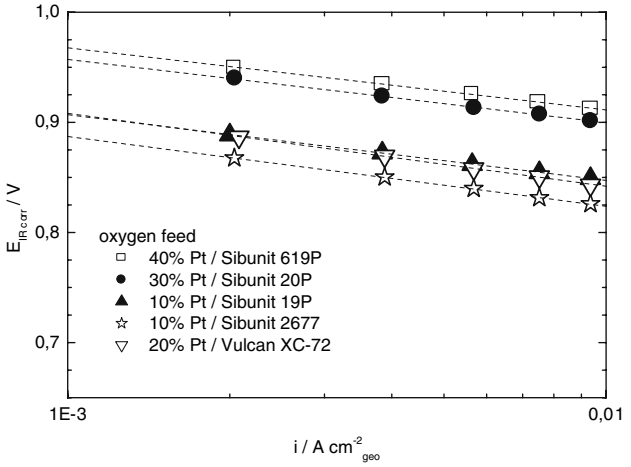

Fig. 6 Tafel plots for the kinetic region of I–U curves of Fig. 4(**b**)

60 °C cell temperature) stipulated by the experimental setup. The Tafel slopes range from 56 mV dec^{-1} (40%Pt/Sibunit 619P) to 66 mV dec^{-1} (10%Pt/Sibunit 2677) reflecting the uncertainty of kinetic data evaluation from full cell measurements. The values of the Tafel slope are in accordance with those reported in the literature for the low overpotential range [25, 29, 31–35].

The resulting values of $\eta_{mt,cat}$ are plotted in Fig. 7a and b for air and for oxygen operated cathodes as a function of the current density. It should be noted, however, that the analysis described above neglects the change in the Tafel slope from ca. 60 to ca. 120 mV dec^{-1} observed below 0.85 V and ascribed to different extents of Pt surface oxidation [31, 33, 34]. Therefore, mass transport losses calculated with Eq. (2) may be overestimated. In the oxygen feed, as expected, mass transport losses at small current densities become practically zero. With increasing current, voltage losses related to mass transport in the oxygen fed cathode reach 81 mV at 1 A cm^{-2} for high surface area 40%Pt/Sibunit 619P and 145 mV for 10%Pt/Sibunit 2677. For air operated cells mass transport losses are naturally higher, ranging from 32 mV for 40%Pt/Sibunit 619P and 68 mV for 10%Pt/Sibunit 19P sample at small current densities to 235 mV at 1 A cm^{-2} and 317 mV at 0.8 A cm^{-2}, respectively.

Furthermore, a qualitative trend can be observed in Fig. 7a and b. With increasing surface area of carbon supports of the Sibunit family, $\eta_{mt,cat}$ decline. Meanwhile, pore distributions indicate a strong increase in the contribution of pores with diameters below 20 nm. We thus speculate that these pores serve as hydrophobic gas diffusion channels supplying oxygen to the surface of Pt particles. This hypothesis allows us to reconcile the differences between Sibunit 20P and Vulcan XC-72, having similar S_{BET} but different $\eta_{mt,cat}$ (especially in the low overpotential region, see Fig. 7a) as well as very different MAs

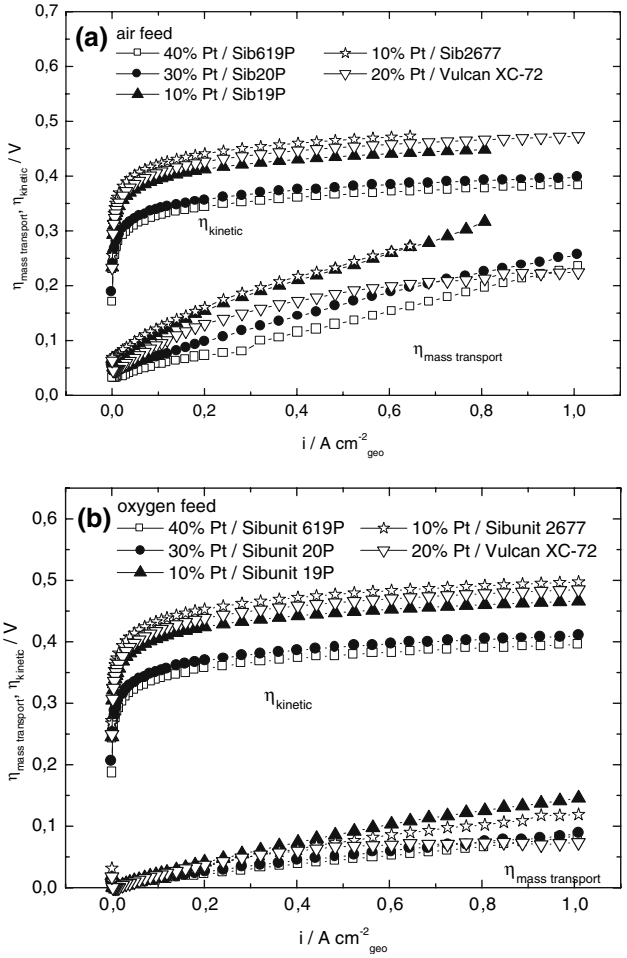

Fig. 7 Kinetic and mass transport overvoltages as a function of current density of air (**a**) and oxygen (**b**) fed cathodes

(Fig. 5). Indeed, as seen from Fig. 1, the contribution of the pores with an average diameter below 20 nm in Vulcan XC-72 is noticeably smaller than in Sibunit 20P and Sibunit 619P, the latter showing the best cathode performance. This hypothesis also helps to explain differences in the support ranking for the anode of liquid fed DMFC [15] and the cathode of the gas fed PEMFC.

Another possible explanation for the improvement in the cathode performance with increasing surface areas of Sibunit supports is the decrease in the ionomer loading per unit surface area of carbon. As observed from Table 2, the Nafion loadings (in mg per m^2 of carbon support) follow the trend of mass transport overvoltages. This can be tentatively attributed to the hindered transport of oxygen to, or product water from, the catalyst particles through the Nafion layer. This second hypothesis, however, is not corroborated by the differences between the cathode catalysts supported on Sibunit and Vulcan. Additional studies on the influence of Nafion content are required to gain better understanding of the influence of carbon support texture on the cathode performance.

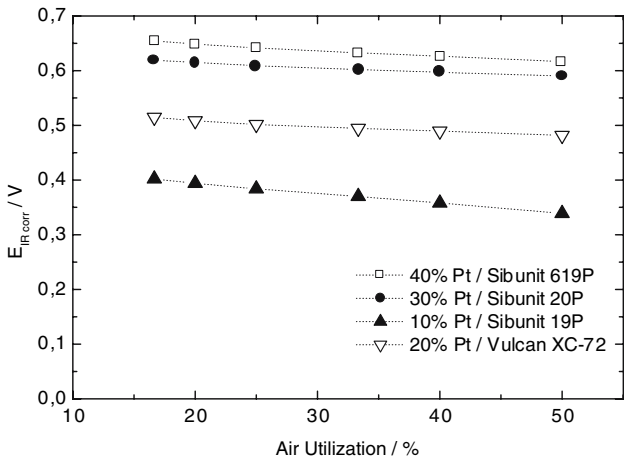

Fig. 8 Utilization curves for cathodes operated with air at 0.6 A cm^{-2} and 60 °C. The cathode with 10%Pt/Sibunit 2677 catalyst gave unstable cell voltages at utilizations higher than 20%

To gain better understanding on the mass transport issues utilization curves were recorded for cathodes fed by air at 0.6 A cm^{-2} (Fig. 8). Here, for the best performing 40%Pt/Sibunit 619P electrode with the lowest Nafion loading per unit surface area of carbon support the cell voltage differs by only 38 mV between 17% (655 mV) and 50% (617 mV) air utilization. On the other hand, for 10%Pt/Sibunit 19P sample with 3.3 mg_{Nafion} m^{-2} stronger dependency on the air utilization or even unstable cell operation were observed.

Although Nafion loadings per unit surface area of carbon for Vulcan XC-72 and Sibunit 20P supported catalysts are very similar, mass transport losses are much higher in the former case. This suggests that mass transport losses are not directly related to the thickness of the Nafion layer on the surface of carbon support but rather to the textural characteristics of the carbon materials, to the balance between hydrophobic and hydrophilic pores and to the interaction between carbon supports and ionomer. We suggest that textural characteristics of the high surface area Sibunit carbons are advantageous for oxygen transport and for water management. Investigations on the ratio of hydrophobic vs. hydrophilic pores in the catalyst layers prepared on the basis of different carbon materials are under way (Volfkovich, unpublished) and will contribute to the understanding of the influence of substructural characteristics of carbon materials on the performance of fuel cell catalysts.

4 Conclusions

In this work we compared Pt catalysts prepared on the basis of carbon supports from the Sibunit family with various degrees of activation and BET surface areas ranging from 22 to 415 m^2 g^{-1} with a conventional 20 wt.%Pt catalyst supported on Vulcan XC-72. Full cell tests revealed a strong influence of the type of carbon support both on the total and mass related currents. The highest mass specific currents at 0.85 V are achieved for 30%Pt/Sibunit 20P and 40%Pt/Sibunit 619P with BET surface areas of carbon supports of 292 and 415 m^2 g^{-1}, correspondingly. These exceed the activities of Vulcan XC-72 supported 20%Pt catalyst by a factor of 4 in the oxygen and 6 in the air feed. The increased mass specific activities cannot be ascribed to the influence of the carbon support on the metal dispersion which was purposely kept constant, and is likely to be due to the improved mass transport and water management in the catalytic layers. A high concentration of mesopores in the range 3–20 nm which serve as hydrophobic gas diffusion channels supplying oxygen to the surface of Pt particles is assumed to improve mass transport in Sibunit carbons.

Acknowledgements The work was supported through the network "Efficient Oxygen Reduction for Electrochemical Energy Conversion" funded by the German Federal Ministry for Education and Science, Grant 01 SF 0302, and partially by the Russian Foundation for Basic Research under Grant 06-03-32737. The authors would like to thank Plaksin G.V. for providing the samples of Sibunit carbons and Voropaev I.N. for assistance in the synthesis of some catalyst samples.

References

1. Vielstich W, Lamm A, Gasteiger HA (eds) (2003) Handbook of fuel cells. Fundamentals, technology and applications. Wiley, Chichester
2. Carrette L, Friedrich KA, Stimming U (2000) ChemPhysChem 1:162
3. Kinoshita K (1988) Carbon. Electrochemical and physicochemical properties. Wiley, New York
4. Uchida M, Aoyama Y, Tanabe M, Yanagihara N, Eda N, Ohta A (1995) J Electrochem Soc 142:2572
5. Uchida M, Fukuoka Y, Sugawara Y, Eda N, Ohta A (1996) J Electrochem Soc 143:2245
6. Xie J, More KL, Zawodzinski TA, Smith WH (2004) J Electrochem Soc 151:A1841
7. Watanabe M, Tomikawa M, Motoo S (1985) J Electroanal Chem 195:81
8. Uchida M, Aoyama Y, Eda N, Ohta A (1995) J Electrochem Soc 142:4143
9. Cui HF, Ye JS, Zhang WD, Wang J, Sheu FS (2005) J Electroanal Chem 577:295
10. Bessel CA, Laubernds K, Rodriguez NM, Baker RTK (2001) J Phys Chem B 105:1115
11. Boxall DL, Deluga GA, Kenik EA, King WD, Lukehart CM (2001) Chem Mater 13:891
12. Steigerwalt ES, Deluga GA, Lukehart CM (2002) J Phys Chem B 106:760
13. Joo SH, Choi SJ, Oh I, Kwak J, Liu Z, Terasaki O, Ryoo R (2001) Nature 412:169
14. Ding J, Chan KY, Ren J, Xiao FS (2005) Electrochim Acta 50:3131

15. Rao V, Simonov PA, Savinova ER, Plaksin GV, Cherepanova SV, Kryukova GN, Stimming U (2005) J Power Sources 145:178
16. Yermakov YI, Surovikin VF, Plaksin GV, Semikolenov VA, Likholobov VA, Chuvilin AL, Bogdanov SV (1987) React Kinet Catal Lett 33:435
17. Barrett EP, Joyner LG, Halenda PP (1951) J Am Chem Soc 73:373
18. Joerissen L, Gogel V, Kerres J, Garche J (2002) J Power Sources 105:267
19. Scherer J (2005) Dissertation. University Ulm, Germany
20. Donnet JB, Bansal RC, Wang MJ (1993) Carbon blacks. Marcel Dekker, New York
21. Kunz HR, Gruver GA (1975) J Electrochem Soc 122:1279
22. Bett J, Lundquist L, Washington E, Stonehart P (1973) Electrochim Acta 18:343
23. Antoine O, Bultel Y, Durand R, Ozil P (1998) Electrochim Acta 43:3681
24. Maillard F, Martin M, Gloaguen F, Leger JM (2002) Electrochim Acta 47:3431
25. Gasteiger HA, Kocha SS, Sompalli B, Wagner FT (2005) Appl Catal B Environ 56:9
26. Simonov PA, Likholobov LA (2003) In: Wieckowski A, Savinova ER, Vayenas CG (eds) Catalysis & electrocatalysis at nanoparticle surfaces, vol 1. Marcel Dekker, New York, p. 409
27. Frenkel AI, Hills CW, Nuzzo RG (2001) J Phys Chem B 105:12689
28. Lundblad A (2004) J New Mater Electrochem Syst 7:21
29. Bernardi DM, Verbrugge MW (1992) J Electrochem Soc. 139:2477
30. Tarasevich MR, Sadkowski A, Yeager E (1983) In: Conway BE, Bockris JOM, Yeager E, Khan SUM, White RE (eds) Comprehensive treatise of electrochemistry, vol 7. Plenum Press, New York, p. 301
31. Damjanovic A (1992) In: Murphy OJ, Srinivasan S, Conway BE (eds) Electrochemistry in transition, vol 102. Plenum Press, New York, p. 107
32. Kinoshita K (1992) Electrochemical oxygen technology. John Wiley & Sons, New York
33. Adzic R (1998) In: Lipkowski J, Ross PN (eds) Electrocatalysis, vol 102. Wiley-VCH, New York, p. 197
34. Gattrell G, MacDougall B (2003) In: Vielstich W, Lamm A, Gasteiger HA (eds) Handbook of fuel cells—fundamentals, technology, applications, vol 2: Electrocatalysis. John Wiley & Sons, Chichester, p. 444
35. Gasteiger HA, Gu W, Makharia R, Mathias MF, Sompalli B (2003) In: Vielstich W, Lamm A, Gasteiger HA (eds) Handbook of fuel cells—fundamentals, technology and applications, ch. 46. John Wiley & Sons, Chichester